ISPRS Annals of the Photogrammetry, Remote Sensing and Spatial Information Sciences, Volume X-5/W4-2025
Philippine Geomatics Symposium (PhilGEOS) 2025 "Enhancing Human Quality of Life through Geospatial Technologies",
24–25 November 2025, Quezon City, Philippines

Comparative Analysis of UAV Photogrammetry and Terrestrial Laser Scanning for 3D Building Reconstruction

Jarence David D. Casisirano[1], Alexis Richard C. Claridades[1]

[1]Department of Geodetic Engineering, University of the Philippines Diliman, Quezon City, Philippines
-{jdcasisirano, acclaridades}@up.edu.ph

Keywords: UAV photogrammetry, TLS, point cloud comparison, 3D building reconstruction, accuracy assessment

Abstract

Recently, unmanned aerial vehicle (UAV) photogrammetry has gained popularity as an alternative to terrestrial laser scanners (TLS) for collecting 3D information, particularly for building models. However, comprehensive comparative assessments of the two methods remain limited in the literature. This study compares TLS and UAV-based photogrammetry for 3D building modeling. 3D point cloud data is collected in a study area using both methods, with ground truth data collected using a total station. The resulting point clouds were evaluated through multiple quantitative metrics, including RMSE, cloud-to-cloud distance, surface area, point density, planarity, roughness, and surface variation, in addition to qualitative assessments of model completeness and feature reconstruction. Results show that TLS achieved lower RMSE and smoother, more accurate facade geometry, particularly in near-ground areas. However, this method failed to capture rooftop structures due to occlusion. The UAV model successfully captured upper structures and finer architectural features but showed noisier surfaces and missing data at the building base. Surface geometry analyses further revealed that TLS outputs were more planar and consistent. Meanwhile, UAV data exhibited greater variation and reconstruction artifacts. The findings highlight the strengths and limitations of each method depending on the modeling objective. While UAV photogrammetry may be sufficient for applications such as solar potential estimation or volume analysis, TLS is more suitable for high-precision tasks like facade documentation or structural monitoring. For projects requiring both accuracy and coverage, a hybrid approach is recommended. This study emphasizes their complementary value and offers guidance for urban-scale 3D data acquisition strategies.

1. Introduction

1.1 Background of the Study

As modern cities rapidly shift toward sustainable and smart infrastructure, digital twins and detailed 3d building models become increasingly important. Ketzler et al. (2020) stated that "3D city model" is still the most prominent term in the field of 3D GIS and that the term "digital twin" has seen a significant increase in academic literature, particularly in the context of cities and built environment studies. Rightfully so, accurate and detailed 3D building models play a pivotal role in many modern geospatial applications, including but not limited to urban planning, infrastructure monitoring, disaster management, and climate change adaptation (Fan et al., 2021; Riaz et al., 2023).

Among the many techniques available to produce accurate 3D building models, terrestrial laser scanners (TLS) and unmanned aerial vehicles (UAVs) are two of the most common. TLS can capture highly accurate, dense, and geometrically reliable point clouds. However, TLS comes with significant challenges, including price, technical know-how, and occlusions brought about by line-of-sight (LOS) limitations. On the other hand, UAV photogrammetry has gained popularity in recent years because of its portability, cost-effectiveness, and ability to rapidly collect data remotely from a range of perspectives (Dominici et al., 2017; Fernández-Hernández et al., 2015). With the emergence of consumer-grade drones, even non-expert users can now generate 3D spatial data with ease. Still, the quality and accuracy of UAV-derived point clouds will vary depending on factors such as camera quality, lighting conditions, target object properties, and flight path designs, to name a few.

While, independently, both technologies are already well established, academic literature discussing the comparative assessment between TLS and UAV photogrammetry is scarce, particularly in the Philippines, where 3D modeling and digital twin technologies are still in the early stages of maturity. Most previous studies focus on less detailed but large-scale 3D mapping using high-end equipment such as Light Detection and Ranging (LiDAR) systems, leaving a gap in understanding how consumer-level UAV systems perform against TLS systems in micro-scale contexts (Santillan et al., 2015; Villanueva et al., 2015). This paper addresses that gap by presenting a case study comparing 3D building point clouds generated using TLS and UAV photogrammetry. The comparison is supported by ground truth data collected via total station measurements.

1.2 Significance of the Study

This study contributes to the growing field of 3D geospatial data acquisition and analysis by providing a head-to-head comparison of TLS and low-cost UAV photogrammetry for building-scale modeling. While TLS has traditionally been viewed as the standard in accuracy and completeness, recent advancements in photogrammetry and drone camera technology suggest that even consumer-grade UAVs can produce, to some extent, competitive results. The findings of this study aim to support geospatial professionals, urban planners, and researchers in selecting appropriate data acquisition techniques for different types of applications. Understanding the trade-offs between these two methods is critical for digital twin development, urban planning, and 3D modeling, especially in contexts where cost, portability, and time constraints are significant considerations. This paper aims to help practitioners and researchers who must balance these competing factors in their workflows make informed decisions.

1.3 Research Objectives

This study aims to evaluate and compare the performance of terrestrial laser scanning (TLS) and UAV photogrammetry in generating 3D building models. It involves generating point

This contribution has been peer-reviewed. The double-blind peer-review was conducted on the basis of the full paper.
https://doi.org/10.5194/isprs-annals-X-5-W4-2025-143-2026

cloud datasets of the same structure using a DJI Mini 3 Pro drone and a terrestrial laser scanner. The study also assesses the accuracy and quality of the UAV-derived point cloud using TLS data and total station measurements as references and evaluates the models based on various spatial metrics. Finally, the study identifies the strengths and limitations of each method in terms of spatial quality and provides recommendations on their suitability for various geospatial modeling applications.

1.4 Review of Related Work

TLS has long been established as a benchmark for acquiring highly accurate and dense 3D data in the built environment (Sternberg et al., 2004). By emitting laser pulses and measuring their returns, TLS can capture precise geometric details with millimeter-level accuracy (Stenz et al., 2020), making it preferred for reliable as-built documentation and structural monitoring. However, it is limited by high equipment costs, restricted mobility, and occlusions from line-of-sight (LOS) obstructions.

In contrast, UAV photogrammetry reconstructs 3D models from overlapping aerial images, with modern software automating image alignment and point cloud generation. Its affordability, ease of deployment, and rapid data acquisition have driven its popularity (Nex et al., 2022) and it has been successfully applied in construction monitoring, disaster response, and archaeology (Dominici et al., 2017; Fernández-Hernández et al., 2015). Compact, consumer-grade UAVs have made 3D spatial data collection more accessible, though quality remains dependent on environmental conditions, image resolution, surface texture, and flight planning. In urban settings, insufficient overlap, motion blur, and narrow-corridor occlusions may produce gaps in the data (Wu et al., 2018).

Both TLS and UAV photogrammetry have proven valuable for 3D building modeling, each with unique strengths. Comparative studies typically evaluate geometric accuracy, completeness, and structural fidelity, using metrics such as cloud-to-cloud (C2C) distance (Kamnik et al., 2019; Liu et al., 2023), root mean square error (RMSE) from ground control points or total station data, point density, completeness, and sometimes roughness, planarity, and volume deviation. Kersten & Lindstaedt (2012) found TLS denser and more accurate, while photogrammetry provided adequate detail for visualization. Fernández-Hernández et al. (2015) showed UAV photogrammetry could produce accurate, interpretable models with sufficient overlap and camera calibration.

Most prior comparisons use high-end UAVs and TLS in open, controlled settings. Fewer assess low-cost drones, which lack RTK modules and are more sensitive to environmental conditions. Micro-scale studies such as on single buildings or in dense urban contexts are especially scarce, particularly in the Philippines. This study addresses these gaps by comparing point clouds from a consumer-grade UAV (DJI Mini 3 Pro) and a TLS unit for a single building in a micro-scale urban context. Ground truth from total station measurements provides an independent accuracy benchmark, offering a practical evaluation of low-cost 3D data acquisition workflows in real-world conditions.

2. Methodology

This section discusses the methodology for this study, as illustrated and summarized in Figure 1.

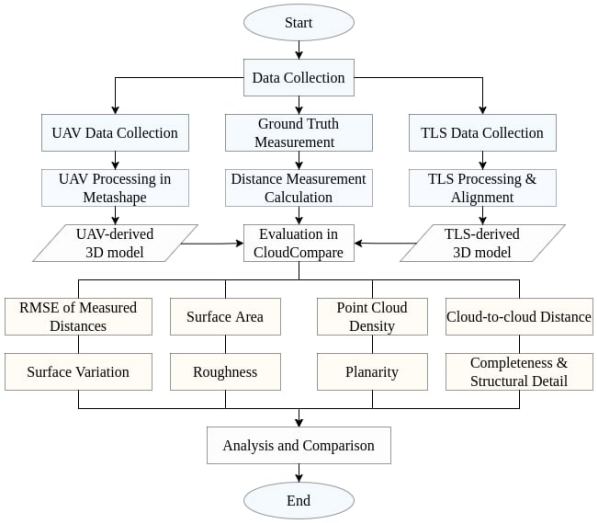

Figure 1. Overall methodology workflow.

2.1 Study Area

The study was conducted at the National Institute of Molecular Biology and Biotechnology (NIMBB), located within the University of the Philippines Diliman campus in Quezon City, Philippines (approximately 14.65072° N, 121.07157° E), as shown in Figure 2.

The building was selected as the target structure due to its well-defined geometry, multiple accessible facades, and relatively clear surrounding space, which are advantageous characteristics for both TLS and UAV photogrammetry. The building is a multi-story facility composed of multiple rectangular artifacts and overhangs. It also has a uniform white paint with trees present in the surrounding area of the building, both of which introduce difficult but necessary challenges in aerial image acquisition and processing. This specific setting reflects common use-case scenarios for 3D building modeling in urban areas using TLS and UAV photogrammetry. It provides a relevant test for evaluating the performance and suitability of low-cost UAV photogrammetry compared to TLS in similar built environments.

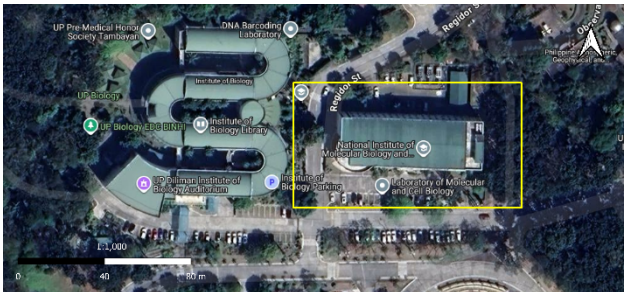

Figure 2. Study area (Google Earth, 2025)

2.2 Data Collection

2.2.1 UAV Data Collection: The data acquisition process for the building followed a segmented approach. The building was divided into five main sections: a nadir (top-down) view of the building and its immediate surroundings and one view for each of the four cardinal sides. As a result, aerial image acquisition was not continuous; the drone was manually repositioned between segments to capture each facade individually. This strategy was necessary due to space limitations and the presence of surrounding trees on all sides of the building, which restricted continuous flight paths. All flights were conducted during favorable weather conditions—either around 10:00 AM or 1:00 PM—under clear skies and bright sunlight, providing adequate illumination for capturing surface details.

Initially, flight automation and pre-programmed waypoints using advanced drone software were heavily considered to streamline data collection. However, this approach proved virtually impossible in practice due to the physical constraints of the study site. The presence of narrow gaps, tight corners, and tree branches extending close to the building walls made it difficult to define safe flight paths with adequate clearance. Furthermore, flight planning involved not only horizontal trajectories for nadir views but also vertical paths for capturing building facades, further complicating the process and increasing operational risk. These challenges, combined with the potential for GPS signal degradation and collision hazards during automated flights, led to the decision to carry out all image acquisition through manual piloting. This approach provided precise control over both drone positioning and camera orientation, thereby ensuring data quality and equipment safety during close-range image captures.

UAV-based imagery was acquired using the DJI Mini 3 Pro, a compact, consumer-grade remotely piloted aircraft (RPA) equipped with a 1/1.3” CMOS camera capable of capturing 48 MP still images. A total of 1,392 images were collected during the mission and distributed across five main building sections: 50 images for the nadir view, 406 for the front facade (south-facing), 527 for the back facade (north-facing), 265 for the right facade (east-facing), and 144 for the left facade (west-facing). The number of images per facade varied due to differences in wall dimensions, drone-to-surface distance, and shooting density driven by on-the-fly overlap estimation.

Because the image acquisition was performed manually, overlap percentages were only estimated based on flight trajectory and shooting intervals. An approximate 60% forward overlap and 60% side overlap were achieved across most segments. Image capture for the facades followed a vertical sweeping approach in which the drone was flown up and down to capture multiple height levels per wall. As a result, the altitude varied continuously throughout this process, in contrast to the nadir segment, which was captured at a relatively constant altitude of approximately 50 meters. Additionally, the drone’s lateral distance from the facades was dynamically adjusted to avoid nearby obstructions, such as tree branches, which posed collision risks. While these adjustments ensured safe proximity and equipment protection, they also contributed to variations in acquisition geometry. Nevertheless, these adaptations were necessary due to the tight spatial constraints and environmental obstructions present at the study site.

2.2.2 TLS Data Collection: TLS data collected from a previous study (Ingles et al., 2024) in the same area was used in this paper. The TLS data collection was conducted using a handheld Foxtech SLAM100 device. It utilizes simultaneous and localization mapping technology for mobile 3D point cloud acquisition. The scanning followed a predefined walking route around the building. One operator carried the scanner, and another monitored the trajectory using the SLAM GO application. A steady walking pace of approximately 5km/h was ensured under clear weather conditions to ensure optimal data quality, and a 60-second initialization phase was completed before scanning. To reduce the noise in the point cloud, the best effort was made to minimize movement during acquisition. This method allowed access to areas difficult to capture using tripod-mounted scanners. However, care was taken to maintain consistent motion and scanner orientation.

2.2.3 Ground Truth Measurements: Ground truth measurements were obtained using a total station (TS). The TS was operated in reflector-less mode, providing an independent reference dataset for evaluating the geometric accuracy of the point clouds generated by UAV photogrammetry and TLS. Establishing a conventional geodetic or project control network using known reference points for TS setup was not feasible for the study due to environmental constraints such as dense vegetation and obstructed sightlines. Instead, the TS was positioned at stable and site-appropriate locations near each building facade. It was operated locally to collect the relative coordinates of identifiable structural features and artifacts, such as building corners and window edges. This process was conducted separately for each facade, resulting in four distinct local coordinate systems—each internally consistent but not references to a global reference network. While this approach did not allow for absolute georeferencing of the ground truth measurements, it enabled the collection of dimensionally valid and reliable measurements within each localized setup. This adaptive methodology, though unconventional, was appropriate for the study’s primary goal of evaluating the geometric fidelity of the 3D reconstructions rather than their absolute positioning. The relative coordinates collected were sufficient for calculating physically meaningful dimensions such as object length and widths used for quantitative assessment of model accuracy in relation to real-world building geometry.

2.3 Processing Workflow

2.3.1 UAV Photogrammetry Processing: First, a custom Python script was used to group the captured UAV images based on the acquisition time stamps, effectively segregating them into five sets corresponding to the nadir view and each of the four building facades. All the UAV photogrammetric data were processed using Agisoft Metashape following a structured and semi-automated workflow. The image groups were imported into separate chunks within the Metashape project to allow for independent processing. Within each chunk, images were aligned using medium accuracy settings that enabled both generic and reference preselection. After alignment, dense point clouds were generated via depth map computation with medium quality and mild filtering. This process was repeated for each of the five chunks. To integrate the datasets, shared markers were manually placed on common architectural features across the chunks for a marker-based chunk alignment. Finally, the chunks were then merged into a unified project while preserving their respective point clouds and tie points.

This contribution has been peer-reviewed. The double-blind peer-review was conducted on the basis of the full paper.
https://doi.org/10.5194/isprs-annals-X-5-W4-2025-143-2026

2.3.2 TLS Point Cloud Integration: The initially unreferenced TLS-derived point cloud was also imported into Metashape as a separate chunk. Using the same marker-based alignment method, it was aligned to the UAV model. Markers were placed on visually identifiable features (e.g., building corners and facade edges) present in both datasets. The alignment was performed without adjusting the scale of the TLS point cloud to ensure that the original dimensions of both the datasets were preserved. This method allowed for a meaningful comparison between the UAV and TLS point clouds.

2.3.3 Ground Truth Data Processing: The ground truth data from the total station contains relative ENZ (Easting, Northing, Elevation) coordinates. Using these coordinates, linear distances between structural features, such as wall lengths and window spans, were computed directly. Although not georeferenced, these measurements were dimensionally accurate and provided a reliable basis for comparing real-world dimensions against those derived from point cloud reconstructions.

2.4 Point Cloud Assessment

The accuracy and quality of the 3D building models were assessed using selected metrics. All evaluations were conducted using CloudCompare, an open-source point cloud analysis platform. The first metric was the completeness assessment. It involved a visual comparison of both datasets to identify missing or occluded regions. Then, the root mean squared error (RMSE) of measured distances was calculated by comparing real-world lengths obtained from total station measurement data with equivalent dimensions extracted from the UAV- and TLS-derived models. Key features such as wall windows and wall lengths were measured. Second, C2C deviation analysis was performed to quantify the spatial differences between UAV and TLS point clouds. The TLS dataset was used as the reference. The statistical outputs were generated to assess consistency across surfaces. Finally, point cloud density was calculated to compare the resolution of each dataset. This calculation provided insight into the level of surface detail captured by each method.

The point clouds were also converted into triangulated mesh models, which were manually segmented by building sections using 3D processing software to calculate surface areas. Planarity, roughness, and surface variation analyses were performed using neighborhood-based geometric descriptors to quantify surface flatness, local texture deviations, and changes in surface normal orientation, respectively. Scalar field visualizations and histograms were used to interpret geometric characteristics. Additionally, a qualitative assessment was conducted by visually inspecting the models' structure, completeness, and mesh quality, with attention to occlusions, artifacts, and fine architectural features. All data processing and analysis were performed using Agisoft Metashape and CloudCompare.

3. Results and Discussion

This section presents a comparative analysis of the 3D data generated from UAV photogrammetry and TLS. These datasets were also evaluated against ground truth data obtained from the total station survey. Quantitative metrics were checked, and qualitative assessments were performed to evaluate geometric fidelity, surface quality, and completeness. These results collectively provide insight into the relative performance and limitations of UAV- and TLS-derived point clouds.

3.1 Visual Comparison of Point Clouds

Figure 3 shows the point clouds produced from UAV photogrammetry and TLS. These outputs exhibit contrasting qualities that reflect their respective acquisition methods. The UAV-derived model captures comprehensive top-down and angled views. It effectively reproduced roof geometry and facade textures with realistic color. However, occlusion due to vegetation and the presence of floating artifacts slightly diminishes its structural definition. On the other hand, the TLS point cloud resulted in clearer wall and base geometry because of its close-range and ground-based acquisition. Still, it suffers from substantial vegetation obstruction, introducing extraneous points, and lacks color information, which limits visual interpretability. These visual and structural differences formed the basis for the succeeding quantitative and qualitative assessments.

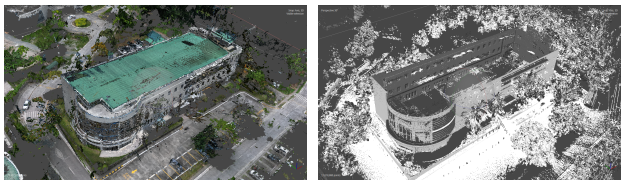

Figure 3. Point clouds derived from UAV (left) and TLS (right)

3.2 RMSE of Measured Distances

A total of 23 architectural features across all the building façades were measured and compared against total station ground truth data to evaluate the dimensional accuracy of the UAV- and TLS-derived point clouds. The resulting overall RMSE is 0.120 meters for the UAV and 0.070 meters for the TLS, as shown in Table 1. The TLS consistently achieved lower absolute errors across most features, especially in horizontal spans such as façade and window widths. These errors indicate that, overall, TLS provided a more accurate representation of real-world distances. For context, previous UAV-based building modeling studies have reported RMSE values as low as 0.015 m when conditions are optimal (Sani et al., 2022).

Facade	UAV RMSE (m)	TLS RMSE (m)
Back Facade	0.1106	0.0601
Right Facade	0.0189	0.0753
Left Facade	0.1216	0.0305
Front Facade	0.1613	0.0882
Overall	0.1195	0.0697

Table 1. RMSE Comparison per Facade

The most pronounced UAV error was recorded on the front facade (0.1613 m), likely due to visual obstructions such as trees near the building entrance. In contrast, the TLS data showed the highest error on the right facade (0.0753 m). However, this is still relatively low compared to UAVs. Interestingly, the left facade showed the most favorable result for TLS (0.0305 m RMSE), possibly due to minimal obstructions and simpler geometry on that side. While the UAV-derived model demonstrated slightly higher RMSE overall, the deviations remained within the commonly accepted tolerance of a few centimeters for building modeling, considering equipment grade and environmental limitations during acquisition (Mirza et al., 2023; Sani et al., 2022). The above results emphasize the strength of TLS in accurate facade reconstruction while also demonstrating the UAV model's adequacy in areas with less occlusion.

3.3 Cloud-to-Cloud (C2C) Distance Analysis

To evaluate geometric alignment between the UAV- and TLS-derived point clouds, a C2C distance analysis was conducted using the TLS dataset as the reference, resulting in the top-down C2C scalar field map in Figure 4 and the histogram of C2C distances shown in Figure 5. While the TLS dataset lacked point coverage for the roof due to its ground-based acquisition perspective, the top-view comparison was still conducted to assess alignment across the building's visible horizontal and upper façade structures. Roof regions in the TLS dataset appear as high-deviation zones in the C2C results; however, these differences are not indicative of modeling errors in either dataset, but rather a direct consequence of occlusion and incomplete overlap. This reinforces the complementary nature of the two methods and highlights the potential benefits of integrating UAV-derived roof data with TLS-acquired facade detail for complete building coverage.

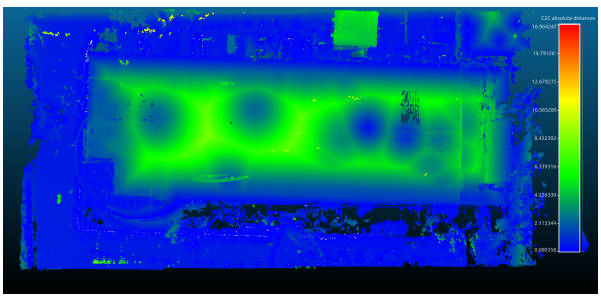

Figure 4. Top View C2C Absolute Distance Visualization

As visualized in Figure 4, most deviations fall within the blue-to-green spectrum. These deviations correspond to sub-meter differences. However, significant deviations were observed in the roof—represented by circular zones with higher C2C values. This result was primarily caused by the TLS dataset lacking point coverage for the roof area, leading to exaggerated discrepancies in those areas when compared to the fully captured UAV model.

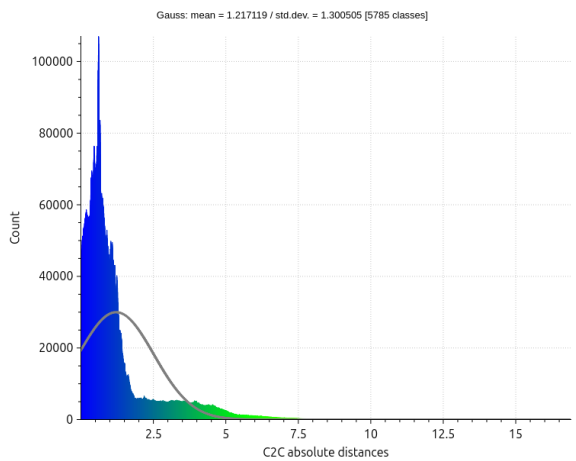

Figure 5. Distribution of C2C Distances between Point Clouds

In contrast, the facade walls exhibit consistent alignment with only minimal variation along vertical surfaces where both datasets have complete overlap. The histogram in Figure 5 confirms this spatial observation. The distribution is right-skewed, with a peak around 1.2 meters and a long tail extending to higher values, further supporting the presence of localized outliers and roof deviations. The computed mean distance of 1.217 m and standard deviation (SD) of 1.301 m reflects moderate geometric variation, primarily due to the absence of TLS data on the roof. Since the TLS scan lacked visibility for elevated horizontal surfaces such as the roof, large discrepancies in those regions are expected and do not necessarily indicate modeling error. Instead, these results underscore the need for integrating complementary datasets when full coverage is required. These results affirm that while both datasets are mostly aligned in the building's primary geometry, further refinement is needed in occlusion-prone zones.

3.4 Point Cloud Density

Surface density analysis reveals significant contrasts between the TLS and UAV-derived point clouds in terms of data resolution, completeness, and spatial coverage. The TLS dataset showed extremely high-density values, particularly concentrated near the scanner's position—primarily at the base of the scan box—where oversampling often occurred, while very few points were captured on the roof. This uneven distribution is a result of the TLS scanner's ground-based position, which leads to dense point capture near the scanner but limited visibility and data loss in higher, occluded areas such as the roof. These patterns underscore the occlusion-sensitive limitation of TLS when used alone for capturing complex vertical structures.

The UAV dataset, as reflected in the surface density distribution shown in Figure 6, demonstrated a more consistent point density overall. Unlike the TLS model, which exhibited a widespread due to localized high-density clusters near the scanner, the UAV point cloud shows a tighter range of values with fewer extreme outliers. This consistency can be attributed to uniform flight coverage and overlapping image acquisition. While the UAV's maximum density was lower than that of TLS, the reduced SD suggests more reliable coverage across the building envelope. However, the density near ground-level facade sections remained limited due to the difficulty of safely piloting the UAV at low altitudes while maintaining sufficient overlap. Overall, the histogram supports the UAV's strength in producing a more balanced and predictable data distribution despite its lower peak density.

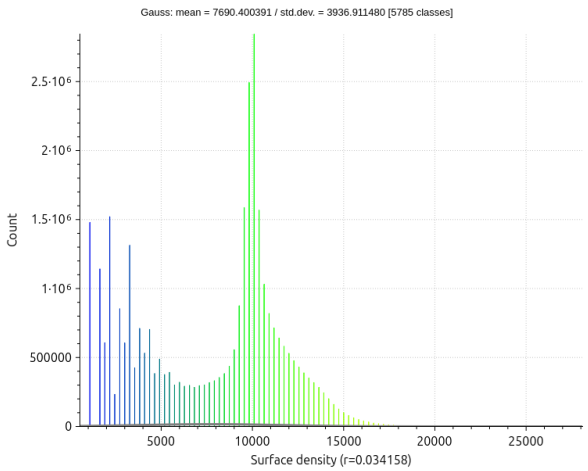

Figure 6. UAV point cloud surface density value distribution

3.5 Surface Area

Surface area measurements for each building section were extracted from both UAV- and TLS-derived meshes and are summarized in Table 2. The UAV model recorded the highest surface area for the roof (1495.11 m²), while the TLS reported no roof data due to its limited vertical field of view. On the facades, the TLS generally produced larger surface areas, notably on the back facade (1007.95 m² TLS vs. 869.67 m² UAV) and right

This contribution has been peer-reviewed. The double-blind peer-review was conducted on the basis of the full paper.
https://doi.org/10.5194/isprs-annals-X-5-W4-2025-143-2026

facade (325.17 m² TLS vs. 256.78 m² UAV). These measurements suggest that the TLS system more effectively captured lower facade sections and vertical geometry, likely due to its closer proximity to the structure. In contrast, the UAV had difficulty capturing near-ground areas, which were affected by altitude restrictions and obstructions such as trees.

Facade	Surface Area (m²) – UAV	Surface Area (m²) – TLS
Front (South)	744.82	774.475
Back (North)	869.668	1007.95
Left (West)	149.944	143.741
Right (East)	256.779	325.168
Roof (Top)	1495.11	0

Table 2. Surface area per facade derived from the point clouds

These discrepancies may also have resulted from residual mesh artifacts and the manual nature of surface segmentation, where boundary delineation was subject to researcher judgment and software limitations. Overestimated values in the TLS model, especially along tree-covered facades, may reflect fused vegetation rather than true wall geometry. Meanwhile, the UAV model likely underestimates facade areas due to missing lower segments. Overall, UAV data performed better in capturing elevated and roof structures, while TLS excelled in vertical and near-ground coverage. This complementarity reinforces the value of integrating both methods for full-envelope structural coverage.

3.6 Local Surface Geometry

3.6.1 Planarity: The planarity analysis for the back facade reveals marked differences between the UAV- and TLS-derived point clouds. As shown in Figure 7, the UAV dataset exhibits a histogram skewed toward higher planarity values. It also has a pronounced peak around 0.73 and an SD of 0.21, indicating that most of its points lie on geometrically consistent flat surfaces.

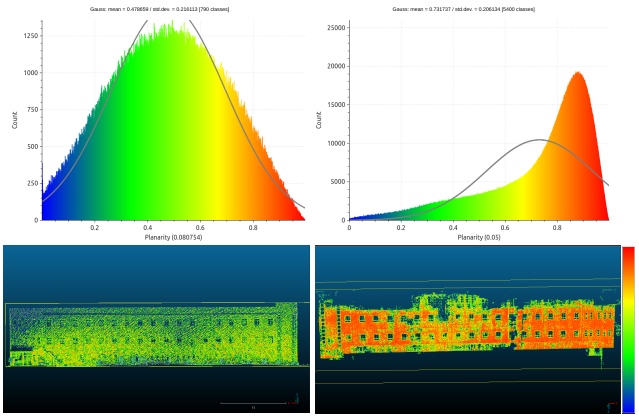

Figure 7. Planarity comparison between TLS and UAV point clouds for the back facade. (Top-left: TLS planarity histogram. Top-right: UAV planarity histogram. Bottom-left: TLS point cloud visualization with planarity scalar field. Bottom-right: UAV point cloud visualization with planarity scalar field.)

This result is visually affirmed by the dense red-to-yellow color gradient in the scalar field map, representing high planarity across large contiguous regions. This result aligns with the UAV's aerial vantage, which facilitates clearer capture of uniform wall structures, especially on unobstructed surfaces like the back facade. In contrast, the TLS dataset yields a histogram with a near-normal distribution centered around a mean planarity of 0.48 and a comparable spread (std. Dev. 0.22). This value suggests a more diverse spread of geometric surface conditions. The corresponding point cloud map reflects this with more scattered mid-range planarity values, particularly in areas near windows and vegetation intrusions at the base. These results emphasize that while TLS provides high-resolution data, it is more sensitive to local structural and textural variations, especially in occluded or cluttered regions, whereas the UAV data benefits from its holistic visibility, producing smoother facade representations in open areas like the building's rear.

3.6.2 Roughness: The comparison of the surface roughness of the back facade, illustrated in Figure 8, reveals a clear distinction between TLS and UAV datasets in terms of localized surface irregularities. Cooler blue tones dominate the TLS-derived point cloud (bottom-left). This result indicates consistently low roughness values across most of the facade surface. This visual uniformity is supported by the TLS histogram (top-left), where values are distributed more broadly but still skewed toward the lower end. The broader spread may reflect geometric details captured by the scanner, such as window frames, vertical edges, and surface protrusions that produce slight variability but do not compromise the overall smoothness of the wall plane.

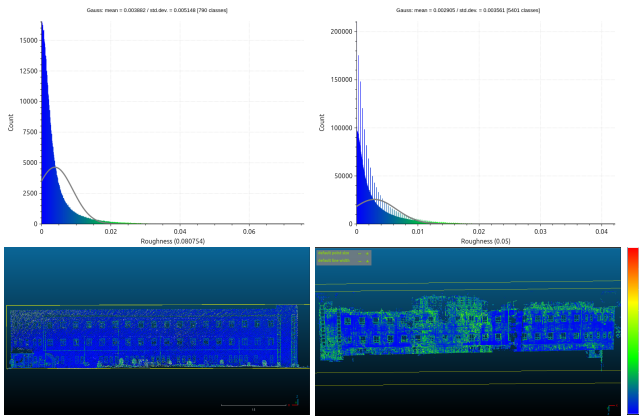

Figure 8. Comparison of surface roughness for the back facade. (Top-left: TLS roughness histogram. Top-right: UAV roughness histogram. Bottom-left: TLS roughness point cloud. Bottom-right: UAV roughness point cloud.)

In contrast, the UAV-derived roughness visualization (bottom-right) exhibits a broader spatial distribution of green and yellow hues, signifying higher roughness in certain regions. This distribution is particularly noticeable in flat wall areas that ideally should be smoother. The UAV histogram (top-right) appears more sharply peaked near zero, yet this statistical concentration hides the rougher appearance in the spatial data. This pattern suggests that while most points have low roughness, the photogrammetric model introduces noise artifacts more visibly across otherwise flat areas. This discrepancy may be due to visual limitations during image matching, particularly in low-texture surfaces. Overall, TLS provides a more visually coherent and geometrically stable surface for the back facade. In contrast, the UAV data, although adequate, shows increased susceptibility to reconstruction noise in smooth, texture-poor surfaces.

3.6.3 Surface Variation: Surface variation is a measure of local geometric complexity and change in normal direction within a neighborhood, providing additional insight into the structural roughness of a point cloud surface. In Figure 9, the TLS dataset (top-left and bottom-left) shows a narrower histogram distribution with a lower mean of 0.0121 and an SD of 0.0266. These values suggest that the TLS point cloud had relatively less

surface variation, indicating more uniform and smoother surfaces on the back facade. This pattern is supported by the TLS point cloud visualization, where the dominant color is deep blue, corresponding to very low surface variation values across most of the wall area.

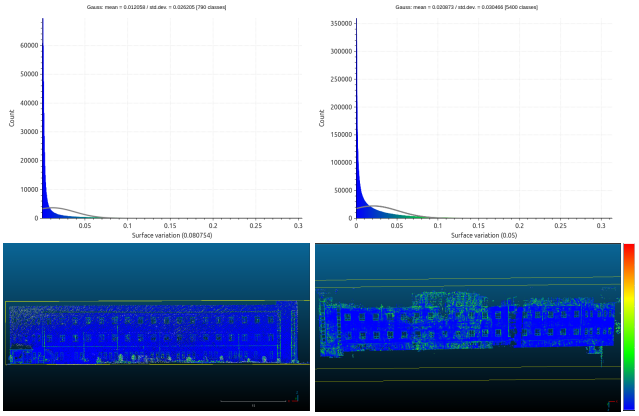

Figure 9. Comparison of surface variation for the back facade. (Top-left: TLS surface variation histogram. Top-right: UAV surface variation histogram. Bottom-left: TLS surface variation point cloud. Bottom-right: UAV surface variation point cloud.)

In contrast, the UAV dataset (top-right and bottom-right) recorded a slightly higher mean of 0.0209 and an SD of 0.0305. These values mean that there is greater variability in local surface orientations of the UAV dataset. While the difference in average values may seem small, it is visually evident in the point cloud visualization, displaying more green tones interspersed with blue. This result is especially true around window edges and other finer architectural features. Understandably, these regions are typically more geometrically complex and more likely to exhibit higher variation in point orientation due to occlusion, reconstruction artifacts, or limitations in image overlap. Nonetheless, the UAV model still captured the overall facade structure with sufficient geometric stability, although with slightly more noise and local irregularities than the TLS model.

3.7 Qualitative Assessment

Visual inspection of the two models offers further qualitative insights into their respective strengths and limitations. The TLS-derived point cloud, though uncolored, exhibits a notably cleaner structure with well-preserved geometric details across the facades. Its strength lies in capturing large-scale architectural elements with minimal noise. The majority of the wall features are also consistently represented. However, the model lacks roof geometry entirely, a direct consequence of occlusion from the ground-based scan position. Smaller features, such as vents, are also difficult to distinguish. On the other hand, the UAV-generated model benefits from photogrammetric colorization, which not only improves visual interpretability but also helps highlight minor surface details like small vents. However, it suffers from greater noise and evident data exclusions at the base of the building—areas where UAV flight paths did not adequately capture low-angle views. Reconstruction accuracy also appears to be affected by surface reflectance and texture. In particular, white or smooth walls, especially on the building's left facade, exhibit patchy reconstruction. Nevertheless, unlike the TLS model, the UAV point cloud successfully includes the full rooftop structure, offering a more complete volumetric representation of the building. These complementary strengths highlight how TLS excels in dense and accurate facade capture, while UAV photogrammetry enhances overall coverage and detail visibility, particularly for higher or occluded elements.

4. Conclusions and Recommendations

This study examined and compared the capabilities of TLS and consumer UAV-based photogrammetry in capturing the geometric features of a multi-facade building. Through a combination of quantitative metrics such as RMSE, C2C distance, surface area, density, planarity, roughness, and surface variation, as well as qualitative visual inspections, we found that both methods have distinct strengths and limitations. TLS produced highly accurate and dense facade models with consistent geometric surface quality, particularly in lower areas close to the scanner. However, it suffered from occlusions, especially in roof sections. Conversely, the UAV-derived point cloud provided more complete coverage of rooftops and upper walls due to its aerial vantage but exhibited increased surface noise and incomplete ground-level detail. It also faced reconstruction difficulties in areas with poor texture or limited visibility.

Despite these differences, the results highlight the potential benefits of a hybrid or targeted approach depending on the specific application. For less detail-sensitive tasks such as solar potential estimation, where capturing the roof structure and general building envelope is more critical than fine facade details and structure, the UAV-derived point cloud may already be sufficient (Han et al., 2020). On the other hand, TLS is more appropriate for applications demanding high geometric accuracy and precision, such as as-built documentation, structural deformation monitoring, or facade conservation, where fine detail, surface smoothness, and accurate scale are essential (Bouziani et al., 2021). Meanwhile, tasks that require both complete coverage and accurate modeling—like heritage digitization or energy modeling—may benefit most from a hybrid method that combines TLS's ground-level precision with UAV's aerial completeness (Le et al., 2022). Established workflows for integrating UAV and TLS datasets typically involve point cloud alignment through iterative closest point (ICP) registration, followed by noise filtering, resolution harmonization (e.g., voxel downsampling), and merging within software platforms such as CloudCompare. These methods leverage UAV's aerial coverage and TLS's detailed façade capture to produce complete, high-accuracy building models. In all cases, aligning the data collection strategy with the intended analytical goals ensures that limitations in either method do not compromise the project outcomes.

To support more consistent and reproducible assessments in future work, we recommend the use of standardized parameter settings for surface geometry metrics, as variations in scale were shown to affect interpretability. If possible, automated feature extraction and measurement tools should also be incorporated to reduce potential human-induced errors. For both TLS and UAV methods, strategic planning of scan positions or flight paths is essential to reduce occlusions and improve completeness. Future studies should also test diverse building forms, materials, and settings to validate results across different urban environments. Ultimately, the selection of a scanning method should be guided by the specific spatial needs and resolution requirements of the project.

Acknowledgments

This work is supported by the PHD Incentive Award (242413 PhDIA Y1), funded by the Office of the Vice Chancellor for

Research and Development (OVCRD) of the University of the Philippines Diliman.

References

Bouziani, M., Chaaba, H., & Ettarid, M., 2021. Evaluation of 3D Building Model Using Terrestrial Laser Scanning and Drone Photogrammetry. *Int. Arch. Photogramm. Remote Sens. Spatial Inf. Sci.* doi.org/10.5194/isprs-archives-xlvi-4-w4-2021-39-2021.

Dominici, D., Alicandro, M., & Massimi, V., 2017. UAV photogrammetry in the post-earthquake scenario: case studies in L'Aquila. *Geomatics, Natural Hazards and Risk*, 8, 103 - 87. doi.org/10.1080/19475705.2016.1176605.

Fan, C., Zhang, C., Yahja, A., & Mostafavi, A., 2021. Disaster City Digital Twin: A vision for integrating artificial and human intelligence for disaster management. *Int. J. Inf. Manag.*, 56, 102049. doi.org/10.1016/j.ijinfomgt.2019.102049.

Fernández-Hernández, J., González-Aguilera, D., Rodríguez-Gonzálvez, P., & Mancera-Taboada, J., 2015. Image-Based Modelling from Unmanned Aerial Vehicle (UAV) Photogrammetry: An Effective, Low-Cost Tool for Archaeological Applications. *Archaeometry*, 57, 128-145. doi.org/10.1111/ARCM.12078.

Google Earth., 2025. *[Satellite imagery of the Nat'l Inst. of Molecular Biology and Biotechnology, Univ. of the Philippines Diliman]* [Online application]. Google. earth.google.com (14 August 2025)

Han, Y., Pan, Y., Zhao, T., and Sun, C., 2019. Evaluating Buildings' Solar Energy Potential Concerning Urban Context Based on UAV Photogrammetry. *Proc. Building Simulation 2019: 16th Conference of IBPSA*, Rome, Italy, 2–4 Sept. 2019, Vol. 16, pp. 3610–3617. doi.org/10.26868/25222708.2019.210902.

Ingles, H. A., Legaspi, A. M. M., Sarmiento, C. J. S., and Claridades, A. R. C., 2024. Accuracy Assessment of a Slam-Acquired Point Cloud Data Using a Variety of Classification Applications, *Int. Arch. Photogramm. Remote Sens. Spatial Inf. Sci.*, XLVIII-4/W8-2023, 307–312, doi.org/10.5194/isprs-archives-XLVIII-4-W8-2023-307-2024.

Kamnik, R., Perc, N., & Topolšek, D., 2019. Using the scanners and drone for comparison of point cloud accuracy at traffic accident analysis. *Accident; analysis and prevention*, 135, 105391. doi.org/10.1016/j.aap.2019.105391.

Kersten, T. P., & Lindstaedt, M., 2012. Automatic 3D object reconstruction from multiple images for architectural, cultural heritage and archaeological applications using open-source software and web services. *Photogrammetrie-Fernerkundung-Geoinformation*, *2012*(6), 727-740. doi.org/10.1127/1432-8364/2012/0152

Ketzler, B., Naserentin, V., Latino, F., Zangelidis, C., Thuvander, L., & Logg, A., 2020. Digital Twins for Cities: A State of the Art Review. *Built Environment*, 46, 547-573. doi.org/10.2148/benv.46.4.547.

Le, H., Van Nguyen, T., Pham, L., Tong, S., Nguyen, L., & Vo, O., 2022. Combined use of Terrestrial Laser Scanning and UAV Photogrammetry in producing the LoD3 of 3D high building model. *Journal of Mining and Earth Sciences*. doi.org/10.46326/jmes.2022.63(4).03.

Liu, J., Willkens, D., Lopez, C., Cortés-Meseguer, L., García-Valldecabres, J., Escudero, P., & Alathamneh, S., 2023. Comparative Analysis of Point Clouds Acquired from a TLS Survey and a 3D Virtual Tour for HBIM Development. *Int. Arch. Photogramm. Remote Sens. Spatial Inf. Sci.* doi.org/10.5194/isprs-archives-xlviii-m-2-2023-959-2023.

Mirza, A., Zakiyon, A., Idris, A., Razali, M., Nasri, M., Ghani, A., & Syafuan, W., 2023. Evaluating the Accuracy of UAV and TLS for 3D Indoor Modelling in Large-Scale Building Environments. *IOP Conference Series: Earth and Environmental Science*, 1240. doi.org/10.1088/1755-1315/1240/1/012003.

Nex, F., Armenakis, C., Cramer, M., Cucci, D., Gerke, M., Honkavaara, E., Kukko, A., Persello, C., & Skaloud, J., 2022. UAV in the advent of the twenties: Where we stand and what is next. *ISPRS Journal of Photogrammetry and Remote Sensing*. doi.org/10.1016/j.isprsjprs.2021.12.006.

Riaz, K., Mcafee, M., & Gharbia, S., 2023. Management of Climate Resilience: Exploring the Potential of Digital Twin Technology, 3D City Modelling, and Early Warning Systems. *Sensors (Basel, Switzerland)*, 23. doi.org/10.3390/s23052659.

Sani, N., Tahar, K., Maharjan, G., Matos, J., & Muhammad, M., 2022. 3D Reconstruction of Building Model Using UAV Point Clouds. *Int. Arch. Photogramm. Remote Sens. Spatial Inf. Sci*. doi.org/10.5194/isprs-archives-xliii-b2-2022-455-2022.

Santillan, J. R., Makinano-Santillan, M., Cutamora, L. C., & Serviano, J. L., 2015. 3D building GIS database generation from LiDAR data and free online web maps and its application for flood hazard exposure assessment. In *36th Asian Conference on Remote Sensing* (pp. 2037-2050). researchgate.net/publication/303486377_3D_Building_GIS_Database_Generation_From_LiDAR_Data_And_Free_Onlineweb_Maps_And_Its_Application_For_Flood_Hazard_Exposure_Assessment (22 October 2025)

Stenz, U., Hartmann, J., Paffenholz, J., & Neumann, I., 2020. High-Precision 3D Object Capturing with Static and Kinematic Terrestrial Laser Scanning in Industrial Applications - Approaches of Quality Assessment. *Remote. Sens.*, 12, 290. doi.org/10.3390/rs12020290.

Sternberg, H., Jahn, I., & Kinzel, R., 2004. Terrestrial 3D Laser Scanning – Data Acquisition and Object Modelling for Industrial As-Built Documentation and Architectural Applications. In 20th ISPRS Congress Technical Commission V (pp. 1012-1017). isprs.org/proceedings/xxxv/congress/comm5/papers/183.pdf (22 October 2025)

Villanueva, J., Ang, M., Inocencio, L., & Rejuso, M., 2015. Semi-Automated Building Footprint Extraction, Delineation and 3D Visualisation of the University of the Philippines Main Campus from LIDAR Data Using GIS-Based Open Source Software, *Proc. FOSS4G Conference 2015, Seoul, South Korea, 14-19 Sept. 2015*, 15, 19. doi.org/10.7275/R5KD1W3F.

Wu, B., Xie, L., Hu, H., Zhu, Q., & Yau, E., 2018. Integration of aerial oblique imagery and terrestrial imagery for optimized 3D modeling in urban areas. *ISPRS Journal of Photogrammetry and Remote Sensing*, 139, 119-132. doi.org/10.1016/J.ISPRSJPRS.2018.03.004.